Creep behavior of TiC$_x$N$_{1-x}$–CoTi cermets synthesized by mechanically induced self-sustaining reaction

A. Morales-Rodríguez [a,*], A. Gallardo-López [a], A. Domínguez-Rodríguez [a],
J.M. Córdoba [b], M.A. Avilés [b], F.J. Gotor [b]

[a] *Departamento de Física de la Materia Condensada, Universidad de Sevilla, Box 1065, 41080 Sevilla, Spain*
[b] *Instituto de Ciencia de Materiales de Sevilla, CSIC-USE, Avda. Américo Vespucio 49, 41092 Sevilla, Spain*

Abstract

The plastic flow of TiC$_x$N$_{1-x}$–CoTi cermets has been investigated by uniaxial compression tests carried out in argon atmosphere at temperatures between 1100 and 1200 °C. Two different cermets, with 5 wt.% W or WC content as sintering additives, have been explored to assess the influence of the sintering additives on creep. The microstructural observations of deformed samples and the mechanical results indicate that the hard phase (ceramic grains) controls the plastic deformation. The stress exponent changes from 1 to 2 with increasing strain rate, suggesting a transition in the deformation mechanism from diffusional creep to grain boundary sliding; both with similar activation energy values of about 400 kJ/mol. This value of activation energy agrees with C diffusion in the carbonitride grains as the strain rate controlling mechanism.
© 2010 Elsevier Ltd. All rights reserved.

Keywords: B. Composites; C. Mechanical properties; C. Creep; E. Cutting tools; Carbonitrides

1. Introduction

Titanium carbonitride-based cermets consist of Ti(C,N) grains with a nickel or cobalt binder percolating the ceramic grains. Their light weight and high values of melting point, hardness, mechanical strength, toughness, thermal conductivity, oxidation and creep resistance make them interesting for substituting conventional hard metals as high speed cutting tool materials.[1] At high speed performance, the tool and workpiece surfaces easily reach temperatures above 1000 °C.[2] Due to this high working temperature, research intended to provide a better understanding of the deformation mechanisms operating at high temperature in this material is required.

Three domains concerning the deformation mechanisms have been observed in hardmetals for cutting tool applications with increasing temperature: brittle, toughness with limited plasticity and creep behavior.[3] Although results relative to the plastic behavior are very scarce, it seems that the deformation is controlled by the carbonitride phase deformation.[4–6]

This research work is devoted to the study of the creep behavior of TiC$_x$N$_{1-x}$–CoTi cermets with two different sintering additives: tungsten (W) and tungsten carbide (WC).

2. Experimental

The Ti(C,N)-based powdered cermets were synthesized in nitrogen atmosphere by a one step mechanically induced self-sustaining reaction (MSR) from the following starting mixture: elemental powders of titanium and graphite (Ti/C atomic ratio of 1/0.5) necessary for the TiC$_x$N$_{1-x}$ formation, 15 wt.% cobalt as binder phase and 5 wt.% metallic W or WC as sintering additives.[7] The local high temperature achieved during MSR synthesis favours the presence of metallic W (even when WC additive is used) instead of a (Ti,W)(C,N) solid solution into the hard phase grains.[7,8] These extreme temperatures reached during MSR process along with the presence of a third metallic phase (W) lead to the formation of a CoTi intermetallic binder phase resulting in a higher C/N ratio of the carbonitride phase than expected.[7] After cold isostatic pressing, the compacts were pressureless sintered at 1400 °C during 1 h in helium atmosphere. Cermets with TiC$_x$N$_{1-x}$ stoichiometry of TiC$_{0.75}$N$_{0.25}$,

* Corresponding author.
   E-mail address: amr@us.es (A. Morales-Rodríguez).

and CoTi + metallic W as binder phase were obtained in both cases. Hereafter the materials will be referred as TiCN–CoTi–W and TiCN–CoTi–WC, respectively. A detailed description of the production method can be found in Ref. [7].

The creep tests were performed on prismatic samples of 2.5 mm × 2.5 mm × 5 mm under uniaxial compression at constant load with stresses ranging from 38 to 103 MPa and temperatures between 1100 and 1200 °C. The creep tests were conducted in argon atmosphere to avoid oxidation of the material. The instantaneous length and time data were continually recorded and then converted and plotted in log $\dot{\varepsilon}$ vs. ε curves, where $\dot{\varepsilon}$ is the strain rate and ε is the nominal strain. These mechanical data were analyzed using the conventional high temperature equation for steady-state creep[9]:

$$\dot{\varepsilon} = A\sigma^n \exp\left(\frac{-Q}{RT}\right), \tag{1}$$

where A is a microstructural parameter which includes the grain size dependence, σ is the true stress, n is the stress exponent, Q is the activation energy for the creep mechanism, R is the ideal gas constant and T is the absolute temperature.

The microstructural characterization of the cermets before and after the creep tests was carried out using a scanning electron microscope – SEM, (JEOL 6450LV, Tokyo, Japan) and a transmission electron microscope –TEM, (Philips CM-200, Eindhoven, The Netherlands), at the CITIUS Microscopy Service, Universidad de Sevilla, Spain. Both microscopes were equipped with microanalysis X-ray energy dispersive spectrometers – EDX (Inca, Oxford Instruments, Abingdon, UK), which allowed chemical analysis of the different phases present in these complex materials. Sections for SEM observations were cut from the samples (sections parallel to the compression axis in the case of deformed specimens) to study the microstructure of the specimens after mechanically polished down to 1 μm. The morphological parameters of the carbonitride grains: equivalent planar diameter, $d = 2(\text{area}/\pi)^{1/2}$, and form factor, $F = (\text{perimeter})^2/(4\pi \times \text{area})$, were measured on SEM micrographs using a semiautomatic image analyzer. Foils for TEM were mechanically thinned from bulk material using conventional techniques: cutting, mechanical polishing, dimpling and a final thinning stage by PIPS (precision ion milling polishing) with Ar ions.

3. Results and discussion

A typical back-scattering SEM micrograph of the as-received TiCN–CoTi–WC cermet is shown in Fig. 1, illustrating the main features of the studied cermets. Both cermets exhibit a homogeneously distributed binder phase (white phase) surrounding the TiCN hard-phase grains (grey phase). Small inclusions of CoTi phase (light grey phase) are observed inside the ceramic grains. A bright white phase mainly located at the ceramic–binder interfaces is also distinguished. The analytical microscopy performed on these segregated grains showed that they correspond to the metallic tungsten reported in the literature for XRD analysis.[7] Some pores are also observed in black color in agreement with 96% nominal densities reported in Ref. [7]. The ceramic skeleton
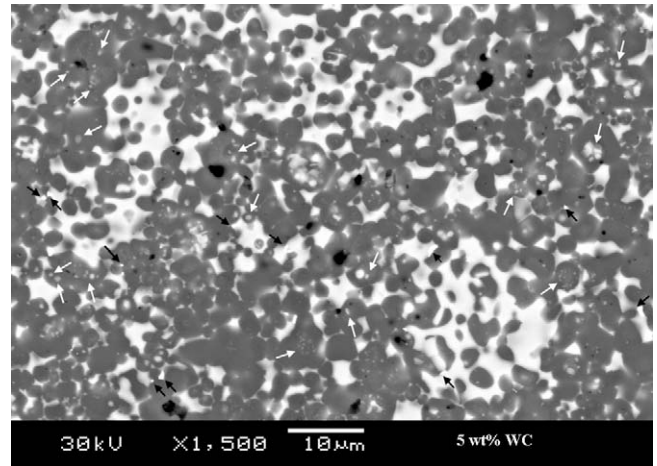

Fig. 1. SEM micrograph using backscattered electrons of the general aspect of the TiCN–CoTi–WC as-received cermet. White and black arrows point to inclusions observed in the TiCN grains and to metallic W segregated at binder-TiCN grain boundaries, respectively. A more detailed explanation can be found in the text.

consists of fairly rounded grains, from which only a negligible percentage showed the typical core-rim structure. A form factor of 0.8 ± 0.1 and average grain size of 1.7 ± 0.9 μm have been measured for both materials. No significant dislocation density is observed inside the carbonitride or binder grains at TEM scale in the as-received samples.

Fig. 2 shows a standard creep curve for TiCN–CoTi–WC cermet at stresses between 39 and 62 MPa and temperatures between 1100 and 1200 °C. Similar values of strain-rate and creep parameters are exhibited by the second TiCN–CoTi–W cermet when deformed at stresses ranging from 54 to 108 MPa at analogous temperature conditions. The average values of stress exponent (n) measured from creep experiments are summarized
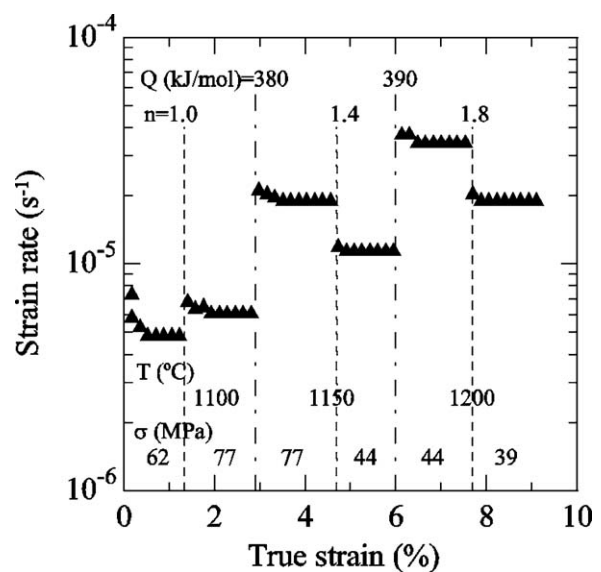

Fig. 2. Typical creep curve plotting strain-rate vs. strain for a sample with WC additive, indicating the stresses and temperatures used. The values of stress exponent and activation energy estimated from the load and temperature changes respectively are also shown.

Table 1
Comparison between stress exponents for the TiC$_x$N$_{1-x}$–CoTi cermets with W and WC additives indicating the analogous temperature conditions and the stresses used for their estimation in each case.

T (°C)	σ (MPa)	Material	n
1100	39–108	TiCN–CoTi–W	1.2 ± 0.2
	48–77	TiCN–CoTi–WC	1.2 ± 0.4
1150	39–89	TiCN–CoTi–W	1.6 ± 0.2
	44–77	TiCN–CoTi–WC	1.6 ± 0.3
1200	38–68	TiCN–CoTi–W	1.8 ± 0.2
	35–44	TiCN–CoTi–WC	1.8 ± 0.2

in Table 1, which shows similar results for both compositions. In the same line, similar average values for activation energy of 380 ± 40 kJ/mol have also been determined for both materials. The values of the stress exponent and activation energies estimated state that there is no dependence of the creep parameters with the starting additive powder composition.

Fig. 3 shows the creep curve of TiCN–CoTi–WC cermet tested at a constant temperature of 1100 °C and stresses ranging between 47 and 100 MPa. The stress exponent increases from 1 to 2 with increasing stress conditions.

The stress exponent tendency, ranging from values close to 1 towards 2 with increasing temperature (Fig. 2) or stress (Fig. 3), suggests a transition in the controlling deformation mechanism within the experimental conditions studied in this work. No signs of macroscopic failure have been observed although the samples were plastically deformed up to 10–12% strain.

No remarkable microstructural features were found at SEM scale after deformation of TiC$_x$N$_{1-x}$–CoTi samples up to 12% strain. For instance, neither deformation of the hard phase grains nor extensive intergranular decohesion has been observed at SEM. The form factor and mean grain size of the deformed carbonitride grains were identical to the values obtained for the as-received materials. Fig. 4a illustrates dislocations observed by TEM inside the metallic CoTi grains. The high local stresses achieved at triple point junctions during creep could be responsible for the dislocations observed in the binder. Several authors[11–13] have already pointed to the generation and move-
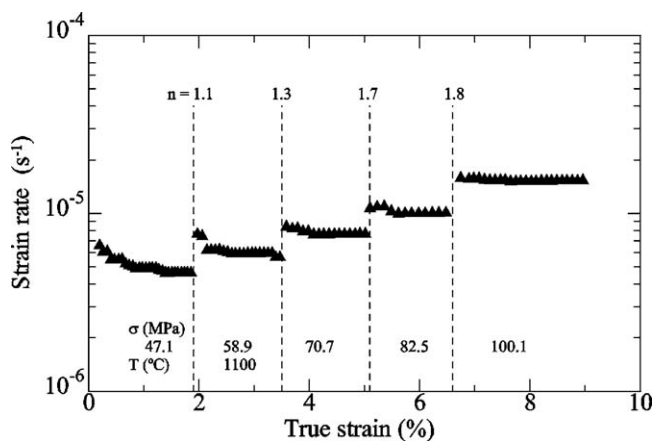
ment of dislocations within the grains as an active mechanism to relax the stress concentration associated to grain boundary sliding in metals and alloys. The regular squared shapes correspond to the binder inclusions inside the carbonitride grains (Fig. 4a). No binder lamellaes otherwise reported in the literature for similar compositions[14] have been observed between the ceramic grains.

Recently, Sakuma and Yoshida[15] have pointed out that TZP ceramics exhibit a strain rate–flow stress relationship (according to the analysis developed by Domínguez-Rodríguez et al.[16]) which results in different domains of n values.

Assuming that the TiC$_x$N$_{1-x}$–CoTi creep behavior is governed by the hard phase, in agreement with other previously studied TiCN-based cermets,[3–6] the microstructural observations together with the mechanical data are consistent with a creep mechanism controlled by diffusion ($n=1$) up to 1100 °C and by grain boundary sliding ($n=2$) above 1200 °C. The previous result indicates that these materials begin to creep by grain boundary sliding motion at higher temperatures than traditional TiCN–Co–Mo$_2$C materials.[6] The progressive change in the stress exponent with increasing strain rate (due to higher temperatures or stresses) observed in this work, indicating a transition from a diffusion-controlled creep to a grain boundary sliding mechanism, agrees with the findings of Ref. [15].

Deformations not larger than 4% were attained under diffusion controlling conditions, therefore no visible grain deformation was revealed by SEM image analysis of the deformed cermets. All creep tests were performed ranging from low to high temperatures or stresses, involving the operation of both deformation mechanisms: diffusion and grain boundary sliding. In order to evaluate the validity of the mechanism transition proposed, a sample was tested under conditions favouring diffusional creep. The cermet was deformed up to 4% strain at strain rates below 3×10^{-6} s^{-1} at 1100 °C under stresses below 50 MPa. Final strain was not large enough to detect any change in the form factor of the ceramic grains from SEM observations.[17] Fig. 4b shows a TEM micrograph of this deformed sample where the binder grains are dislocation-free as well as the TiCN phase. This result agrees with a diffusional creep regime where deformation takes place due to the mass transport of vacancies along grain boundaries, so that no stress concentration occurs at these grain boundaries and therefore dislocations are no longer necessary to accommodate the deformation mechanism.

In the temperature range studied in this work, which corresponds to a CoTi-homologous temperature range of (0.85–0.92) T_m,[10] extensive plastic deformation of the binder is expected at high rates, allowing us to rule out the intermetallic as the rate-controlling phase. Focusing on the ceramic phase, the carbon and titanium diffusivities in TiC have been extensively studied by Sarian.[18,19] The reported Q values for C and Ti self-diffusion in TiC are 400 kJ/mol[18] and 740 kJ/mol[19] respectively. The activation energies measured for these TiC$_x$N$_{1-x}$–CoTi cermets are therefore in agreement with carbon diffusion as the rate-controlling mechanism. The microstructural observations indicate that dislocations may also act as an accommodation mechanism in the studied cermets together with diffusion during grain boundary sliding deformation processes, though this

Fig. 3. Creep curve of a TiCN–CoTi–WC cermet tested at 1100 °C. The stress range explored and the values of stress exponent determined from the load changes are indicated in the plot.
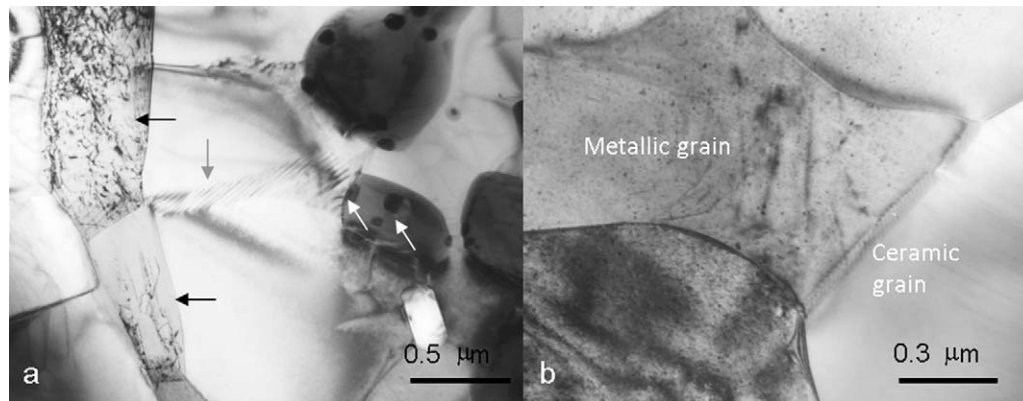
Fig. 4. (a) TEM micrograph of a TiCN–CoTi–WC sample deformed under high stresses to a 12% strain showing dislocations inside metallic grains (indicated by black arrows). The ceramic grain displays a low angle grain boundary (indicated by a vertical grey arrow) and binder inclusions (some of them are indicated by white arrows), most of them with a characteristic squared shape and smaller W rounded inclusions. These inclusions tend to concentrate on the grain surface. (b) TEM micrograph of a TiCN–CoTi–W sample deformed only at low stresses and up to 5% strain showing a neglectable amount of dislocations in the metallic grains. This microstructure corresponds to a diffusional creep stage, with a stress exponent $n = 1$.

latter mechanism, the slowest, is the one which controls the strain-rate.

4. Conclusions

In conclusion, TiC_xN_{1-x}–CoTi cermets, synthesized using two different sintering additives: tungsten (W) and tungsten carbide (WC) respectively, have been creep tested showing no remarkable differences in their mechanical behavior at high temperatures.

The TiCN phase controls the plastic deformation, which evolves from diffusional creep to grain boundary sliding as strain rate (stress or temperature) increases. Both deformation mechanisms are rate-controlled by the carbon self-diffusion in the TiCN phase. The temperature range at which the grain boundary sliding motion controls the plastic behavior exceeds 1150 °C, which allows us to conclude that these TiC_xN_{1-x}–CoTi cermets exhibit an improved resistance to extended plastic deformation.

References

1. Zhang S. Titanium carbonitride-based cermets: processes and properties. *Mater Sci Eng A* 1993;**163**:141–8.
2. Lin J, Liu CY. Measurement of cutting tool temperature by an infrared pyrometer. *Meas Sci Technol* 2001;**12**:1243–9.
3. Mari D, Bolognini S, Feusier G, Viatte T, Benoit W. Experimental strategy to study the mechanical behaviour of hardmetals for cutting tools. *Int J Refract Met Hard Mater* 1999;**17**:209–25.
4. Okuyama K, Sakuma T. High temperature plastic flow in TiC–20 wt%Mo₂C–20 wt%Ni cermet. *Mater Sci Eng A* 1995;**194**:63–8.
5. Cutard T, Viatte T, Feusier G, Benoit W. Microstructure and high temperature mechanical properties of $TiC_{0.7}N_{0.3}$–Mo₂C–Ni cermets. *Mater Sci Eng A* 1996;**209**:218–27.
6. Bolognini S, Feusier G, Mari D, Viatte T, Benoit W. High temperature mechanical behaviour of Ti(C,N)–Mo–Co cermets. *Int J Refract Met Hard Mater* 1998;**16**:257–68.
7. Córdoba JM, Alcalá MD, Avilés MA, Sayagüés MJ, Gotor FJ. New production of TiC_xN_{1-x}-based cermets by one step mechanically induced self-sustaining reaction: powder synthesis and pressureless sintering. *J Eur Ceram Soc* 2008;**28**:2085–98.
8. Lavergne O, Robaut F, Hodaj F, Allibert CH. Mechanism of solid-state dissolution of WC in Co-based solutions. *Acta Mater* 2002;**50**:1683–92.
9. Poirier J. Creep of crystals. In: *High-temperature deformation processes in metals, ceramics and minerals.* 1st ed. Cambridge: Cambridge University Press; 1985.
10. Murray JL. The Co–Ti (cobalt–titanium) system. *Bull Alloy Phase Diagr* 1982;**3**:74–85.
11. Ball A, Hutchison MM. Superplasticity in the aluminum–zinc entectoid. *Met Sci J* 1969;**3**:1–7.
12. Arieli A, Mukherjee AK. A model for the rate-controlling mechanism in superplasticity. *Mater Sci Eng A* 1980;**45**:61–70.
13. Langdon TG. A unified approach to grain boundary sliding in creep and superplasticity. *Acta Metall Mater* 1994;**42**:2437–43.
14. Östberg G, Buss K, Christensen M, Norgren S, Andrén H, Mari D, et al. Mechanisms of plastic deformation of WC–Co and Ti(C,N)–WC–Co. *Int J Refract Met Hard Mater* 2006;**24**:135–44.
15. Sakuma T, Yoshida H. High temperature grain boundary plasticity in ceramics. *Mater Trans* 2009;**50**:229–35.
16. Domínguez-Rodríguez A, Gómez-García D, Castillo-Rodríguez M. A critical assessment of the dislocation-driven model for superplasticity in yttria tetragonal zirconia polycrystals. *J Eur Ceram Soc* 2008;**28**:571–5.
17. Gómez-García D, Domínguez-Rodríguez A, de Portu G. A first study of the high-temperature plasticity of ceria-doped zirconia polycrystals. *J Eur Ceram Soc* 2010;**30**:3357–62.
18. Sarian S. Anomalous diffusion of ¹⁴C in $TiC_{0.67}$. *J Appl Phys* 1968;**39**:5036–41.
19. Sarian S. Diffusion of ⁴⁴Ti in TiC_x. *J Appl Phys* 1969;**40**:3515–20.